HHS Public Access

Author manuscript

Glia. Author manuscript; available in PMC 2019 July 09.

Published in final edited form as:

Glia. 2016 March ; 64(3): 440–456. doi:10.1002/glia.22939.

Astrocytes Spatially Restrict VEGF Signaling by Polarized Secretion and Incorporation of VEGF into the Actively Assembling Extracellular Matrix

Kristof Egervari[1,*], **Gael Potter**[1,*], **Maria Luisa Guzman-Hernandez**[2], **Patrick Salmon**[1], **Martinho Soto-Ribeiro**[3], **Birgit Kastberger**[3], **Tamas Balla**[2], **Bernhard Wehrle-Haller**[3], and **Jozsef Zoltan Kiss**[1]

[1]Department of Neurosciences, University of Geneva, Switzerland [2]Section on Molecular Signal Transduction, Program for Developmental Neuroscience, Eunice Kennedy Shriver National Institute of Child Health and Human Development, National Institutes of Health, Bethesda, Maryland [3]Department of Cell Physiology and Metabolism, University of Geneva, Switzerland.

Abstract

The spatial organization of vascular endothelial growth factor (VEGF) signaling is a key determinant of vascular patterning during development and tissue repair. How VEGF signaling becomes spatially restricted and the role of VEGF secreting astrocytes in this process remains poorly understood. Using a VEGF-GFP fusion protein and confocal time-lapse microscopy, we observed the intracellular routing, secretion and immobilization of VEGF in scratch-activated living astrocytes. We found VEGF to be directly transported to cell-extracellular matrix attachments where it is incorporated into fibronectin fibrils. VEGF accumulated at β1 integrin containing fibrillar adhesions and was translocated along the cell surface prior to internalization and degradation. We also found that only the astrocyte-derived, matrix-bound, and not soluble VEGF decreases β1 integrin turnover in fibrillar adhesions. We suggest that polarized VEGF release and ECM remodeling by VEGF secreting cells is key to control the local concentration and signaling of VEGF. Our findings highlight the importance of astrocytes in directing VEGF functions and identify these mechanisms as promising target for angiogenic approaches.

Keywords

extracellular matrix; fibrillar adhesion; fibronectin; growth factor signaling

Address correspondence to Prof. Jozsef Zoltan Kiss, MD, Department of Fundamental Neurosciences, University of Geneva Medical School, Rue Michel-Servet 1, CH-1211 Geneva 4, Switzerland. Jozsef.kiss@unige.ch.

*Kristof Egervari and Gael Potter contributed equally to this work.

The authors have no conflicts of interest to declare.

Additional Supporting Information may be found in the online version of this article.

Introduction

The vascular endothelial growth factor-A (VEGF) is expressed as a balanced mixture of long, extracellular matrix (ECM) associated (VEGF-189 and 206), intermediate (VEGF-165), and diffusible, short (VEGF-121) isoforms (Carmeliet and Ruiz de Almodovar, 2013; Ferrara, 2010; Houck et al., 1991; Wijelath et al., 2002). VEGF has received great attention due to its pivotal role in angiogenesis (Ferrara, 2002a,b), however, in the nervous system it is rather multifunctional, and has been widely implicated in development, tissue maintenance as well as repair (Carmeliet and Ruiz de Almodovar, 2013). VEGF regulates neurogenesis (Jin et al., 2002; Schanzer et al., 2004; Sun et al., 2003), neuronal survival (Ruiz de Almodovar et al., 2009; Tolosa et al., 2008; Van Den Bosch et al., 2004), migration of microglial cells (Ryu et al., 2009), neurons (Ruiz de Almodovar et al., 2010), glial (Learte et al., 2008), and progenitor cells (Hayakawa et al., 2011; Zhang et al., 2003) as well as neuronal plasticity (Huang et al., 2012; Licht et al., 2010, 2011). Among the many cell types that express VEGF in the brain, post-lesional VEGF secretion by the reactive glia has gained special attention (Ijichi et al., 1995; Li et al., 2014; Margaritescu et al., 2011; Pichiule et al., 1999). After hypoxic/ischemic damage, astrocyte-derived VEGF not only stimulates angiogenesis as well as endothelial cell proliferation, but also has a protective and trophic effect on neurons (Sondell et al., 1999; Zachary, 2005). However, excessive VEGF secretion by the reactive glia could become deleterious by disrupting the blood brain barrier (Argaw et al., 2012). Similar adverse effects limit the application of recombinant VEGF to promote revascularization after ischemic brain injuries (Manoonkitiwongsa et al., 2006).

The actual outcome of VEGF signaling on cellular activities can be highly context dependent. Targeted VEGF secretion and interactions between VEGF signaling elements and the ECM could play an important role in the spatiotemporal coordination of VEGF actions (Ashikari-Hada et al., 2005; Chen et al., 2010; Jakobsson et al., 2006; Ruhrberg et al., 2002; Traub et al., 2013; Wijelath et al., 2002, 2006). However, little is known about the regulation of such interactions and the role of VEGF secreting astroglial cells in this process. Here we set out to investigate the intracellular trafficking, mode of secretion and ECM interactions of VEGF in polarized astrocytes. We took advantage of a VEGF-GFP fusion protein (Guzman-Hernandez et al., 2014) to follow the distribution of VEGF-165 during its trafficking in primary cells. We demonstrate a targeted secretion, astrocyte-dependent incorporation to the ECM and endocytosis-based elimination of VEGF-165 at integrin-mediated fibrillar adhesion sites. Moreover, we show that cell-derived, matrix-bound VEGF but not soluble VEGF, decreases β1 integrin turnover in fibrillar adhesions, suggesting that a spatially restricted VEGF activity might be required to regulate VEGF functions during regeneration.

Materials and Methods

All animal experiments were conducted in accordance with Swiss laws, previously approved by the Geneva Cantonal Veterinary Authority.

Lentiviral Vectors

The Gateway recombination technology (Invitrogen) was used to subclone GFP, mCherry, VEGF-GFP (Guzman-Hernandez et al., 2014) and the β1-SNAP constructs into pCLX lentiviral vectors after the ubiquitin promoter. Lentiviral vectors were produced, concentrated as previously described (Salmon, 2013).

Primary Mixed Cultures of Neuronal and Glial Cells, Transduction, Wounding, and Live Staining of SNAP-Tag

Postnatal day 0-1 Wistar rat cerebral cortices were separated from the subventricular zone by dissection, and after mechanical dissociation cells were plated onto poly-L-lysine (Sigma) and fibronectin (10 μg/ mL, Biopur) coating. At day *in vitro* 3, cultures were transduced with lentiviruses with multiples of infection 1–3 (>75% efficiency). Cultures were grown until confluence in Dulbecco's modified Eagle's medium (Sigma) with 10% fetal calf serum and 1% penicillin-streptomycin, and then medium was changed to serum-free Neuro-basal (Gibco) medium supplemented with 2% B27 (Gibco), 2 mM glutamate, 1 mM sodium pyruvate, 2 mM *N*-acetyl-cysteine, and 1% penicillin-streptomycin. Twenty-four hours later straight scratches of ~ 150 μm width were made, and cells were grown for another 12-24 h before experiments. For live staining of β1-SNAP, SNAP-Surface 549 (1/750, New England Biolabs) was applied for 30 min at 37°C.

Immunofluorescence, Phalloidin Staining, and Image Acquisition

Immunostaining of cell cultures and cryostate sections was performed as described previously (Vutskits et al., 2001). For phalloidin staining of actin filaments, cells were incubated 20 min RT with phalloidin-Alexa568 (Life Technologies, 1/40) following the incubation with secondary antibodies. Images were acquired with a Nikon Eclipse 80i (Nikon Instruments) epifluorescent microscope, with an LSM 510 META (Carl Zeiss) and a Nikon A1 (Nikon Instruments) laser scanning confocal microscope. Image processing was carried out with the NIS-Elements Advanced Research platform (Nikon Instruments, version 3.21.0), and the Metamorph Software (Molecular Devices, version 7.4).

Quantifications of Post Hoc *Experiments*

Quantification of cellular polarization was performed as previously described (Etienne-Manneville and Hall, 2001). For quantifications of the polarized distribution of VEGF-GFP randomly captured epifluorescent images of the wound edge of VEGF-GFP transduced cultures were analyzed comparing regions of interests (ROI) at "leading edge," "center" (excluding the Golgi), "trailing edge." For some experiments, nocodazole (1 μg/ml for 16 h, Sigma) or equivalent quantities of DMSO was added to the culture at wounding and ROI were compared. To quantify VEGF-GFP intensity at adhesions, using confocal images of wound edge astrocytes immunostained against or FN, or for ec. FN masks were determined: (1) positive regions ("at"), (2) regions surrounding in a 3 μm band the positive regions ("around"), and (3) negative regions ("elsewhere"). GFP intensity was measured in the three masks. For BrdU experiments, low density cultures were pulse labeled for 1 h with BrdU (30.75 μg/ml), cell counts were performed after immunostaining (anti-BrdU, anti-Ki67):

BrdU1 and Ki67+ cells in the GFP1 population, and finally BrdU1 cells in the Ki67+/GFP+ population.

Quantifications of Live Experiments

Time-lapse with dynasore or puromycin.—Twelve hours after wounding, VEGF-GFP and β1-SNAP coexpressing astrocytes were imaged in a confocal scanning time-lapse microscope (1.75–7 min/ frame) focusing on cellular adhesions. Dynasore (80 μM, Sigma) or equivalent quantities of DMSO was applied during imaging, and at some experiments washed out was performed with medium+DMSO. GFP intensity of ROIs at VEGF accumulated adhesion areas were measured in time. Puromycin (10 μg/ml, Sigma) was added to the cultures >140 min after imaging, and was washed out 270 min later. Whole cell and background fluorescence of both VEGF-GFP and β1-SNAP was measured. VEGF-GFP was also corrected for interacquisition photobleaching by normalization for intensities of deposited VEGF complexes.

Fluorescence recovery after photobleaching.—VEGF-GFP or GFP and β1-SNAP coexpressing cultures were imaged in a confocal time-lapse microscope. Following 3 min of 10 s/frame prebleach imaging, 3 μm, circular ROIs at adhesions were bleached for 5 s, and imaging was continued for 15 min at 10 s/frame*. Fluorescence intensity was measured at bleached adhesions, and with the easy-FRAP (Rapsomaniki et al., 2012) background was subtracted, data points were normalized for prebleach intensities and corrected for photobleaching using whole cell fluorescence. Fractional fluorescence recovery curves were individually fitted using a double exponential model to obtain the Mobile Fraction (MF). Experiments were also performed on control cells before and after addition of 200 ng/ml human recombinant VEGF-165 (PeproTech).

A detailed description of the methods applied in this study is available as Supporting Information.

Results

Green Fluorescent Protein-Tagged VEGF-165 Shows a Vectorial Distribution in Polarized Astrocytes In Vitro

To investigate the subcellular targeting of VEGF in polarized astrocytes *in vitro,* we used a VEGF-GFP fusion protein encoding the ECM-binding human isoform, VEGF-165, which is commonly upregulated after injury (Fig. 1A). The functional characterization in our previous study (Guzman-Hernandez et al., 2014) demonstrated that VEGF-GFP was secreted comparable to wild type VEGF and it retained biological activity in COS7 cells (Guzman-Hernandez et al., 2014). Colocalization of the GFP and anti-VEGF signals (Supp. Info. Fig. 1A) showed that the fusion protein remained intact and hence could be used to study VEGF localization. We induced cellular polarization and migration in a wound-healing model (Etienne-Manneville and Hall, 2001; Fig. 1B) on primary mixed-glial cultures containing high numbers of GFAP+ astrocytes (Fig. 1B, insert). Twenty-four hours after the scratch, cultures transduced with VEGF-GFP lentivectors were fixed and immunostained. Although not strictly comparable to the polarity of astrocytes *in vivo* (i.e., vascular endfeet,

perisynaptic astrocytic processes, or perilesional orientation), we could observe *in vitro* astrocytic polarization based on Golgi (GM130) and centrosome (γ-tubulin) reorganization toward the wound. Polarized morphology was acquired in 75% of wound edge astrocytes (Supp. Info. Fig. 1B,C). In polarized cells, VEGF-GFP was found at the Golgi (Fig. 1C, insert II.), while a prominent apical accumulation of dot-like GFP1 particles was also observed at the wound edge (Fig. 1C). The VEGF positive apical zone was usually close to the leading edge, but always sparing the peripheral zone of actin arcs (Supp. Info. Fig. 1D, dotted line). Quantifications (Fig. 1D) demonstrated that this vectorial distribution of VEGF-GFP was commonly present after polarization. By disrupting microtubules, Nocodazole treatment (1 μg/ml for 16 h) severely affected the leading-edge accumulation of VEGF in wound edge astrocytes (Fig. 1E) and equalized the distribution of GFP fluorescence (Fig. 1F). These observations suggested that the VEGF fusion protein used a microtubule-dependent directional transport to reach the leading edge of polarized astrocytes.

Based on the enrichment of VEGF-GFP close to the wound edge, we hypothesized that VEGF might be actively directed to integrin-dependent attachment points between the cell and the underlying matrix. To test this, we immunostained fixed VEGF-GFP expressing astrocytes with antibodies against vinculin (Vin, a marker for focal adhesions) and fibronectin (FN, which labels cell-derived ECM and α5β1 integrin containing fibrillar adhesions). Confocal analysis revealed that a good fraction of the GFP signal was localized close to Vin patches and FN fibrils, even beyond the apical areas (Fig. 2A). Moreover, FN/VEGF-GFP (Fig. 2A, insert I., arrowheads), or less frequently FN/Vin/VEGF-GFP triple colocalizations (Fig. 2A, insert I., arrow) were also apparent. A closer inspection revealed, that VEGF was located mainly at the more mature, FN fibril-containing proximal end and rarely at the Vin1 distal aspect of individual cell-matrix adhesions (Fig. 2A, insert II.). Quantifications confirmed these visual observations, as the average GFP intensity at Vin patches (“at”) was only mildly higher than GFP intensity 3 μm “around” Vin patches, or at the rest of the cell (Golgi excluded, “elsewhere”; Fig. 2B), while the mean GFP intensity was significantly higher “at” FN+ fibrils than “around” or “elsewhere” (Fig. 2C) in the cells. Thus, at least part of VEGF-GFP was directed to cell-matrix adhesions.

To investigate whether VEGF accumulates in intracellular vesicles or outside the cell associated with the ECM, we used a two-step immunostaining protocol (Fig. 3A, schematic) with antibodies applied first on living, then on fixed/ permeabilized cells, thereby discriminating extracellular (ec.) from intracellular VEGF-GFP pools (total GFP+/ec. GFP-). Astrocytes stained extensively with ec. GFP, which indicated that a large proportion of astrocyte-derived VEGF is located in the ec. space, strongly colocalizing with FN fibrils. Despite the limited penetration of antibodies to the cell-attachment areas under cells, ec. GFP and ec. FN fibrils showed a clear trend to colocalize (Fig. 3A, arrowheads), as underlined also by the significantly higher average ec. GFP intensity “at” ec. FN+ areas (Fig. 3B). Based on these observations we concluded that VEGF-GFP associated with FN-containing ECM fibrils assembled at fibrillar adhesions. Interestingly, ec. GFP accumulating at cell-cell junctions was not colocalizing with ec. FN (Fig. 3A, arrows).

To better evaluate the localization of VEGF on the cell surface, we performed electron microscopic analysis on cells after pre-embedding DAB-labeling against ec. GFP. VEGF-

GFP aggregates of variable thickness were found closely apposed to the cell surface (Fig. 3C, arrow at left), reflecting sequestration within the ec. fibronectin network. Moreover, VEGF-GFP also covered vesicles or cell protrusions shedding from the cell surface (Fig. 3C, arrows at right), showing the presence of this unique way of VEGF delivery in astrocytes, similarly to what was observed previously in COS7 cells (Guzman-Hernandez et al., 2014). Importantly, when cells were chased at 37°C following ec. antibody incubation, we found DAB labeled GFP also in membrane proximal, intracellular vesicles, reminiscent of caveolae (Fig. 3D). These observations indicated that VEGF is associated with the ECM, shed from the plasma membrane on vesicles or endo-cytosed by cells.

Together, these findings lend strong support to the hypothesis that there is a directional transport of VEGF-GFP toward the cell periphery with subsequent incorporation to the ECM at cell-matrix adhesion sites.

Dynamics of VEGF-GFP in Actively Assembling ECM

To investigate dynamic aspects of VEGF accumulation on the cell surface, we performed time-lapse confocal imaging of mCherry (to visualize the whole cell) and VEGF-GFP cotransduced cell cultures (10 min/frame, Fig. 4A, Movie 1). We found that the localization of VEGF accumulations was changing synchronously with cell movements, such that in cells stretching into the wound VEGF-GFP dots appeared transiently at the leading edge and more stable VEGF accumulations were formed only at substrate-anchorage regions (Movie 1, dashed circles and Fig. 4A, arrowheads of all colors). If a cell-matrix anchorage site was released, the VEGF signal quickly disappeared (Movie 1, dashed square). At some accumulation sites VEGF-GFP dots coalesced into parallel stripes (Movie 1, arrows), resembling the formation of FN-fibrils at sites of fibrillar adhesions.

During maturation of cell-matrix adhesions, FN-bound integrins are pulled inwards as a result of actomyosin contraction. During this process, globular, soluble FN is bound to integrins and then stretched to promote lateral association to form FN fibrils on the cell surface (Fig. 4B, schematic), which process is also known as ECM remodeling (Pankov et al., 2000; Zamir and Geiger, 2001). To analyze the dynamics of VEGF with maturing FN fibrils in fibrillar adhesions, we imaged inwards “sliding” adhesions on astrocytes coexpressing VEGF-GFP and a live stained, SNAP-tagged β1 integrin (β1-SNAP; Fig. 4B). We observed that VEGF-GFP dots first appeared near the distal aspect of β1 integrin containing cell-matrix adhesions, which were subsequently covered with VEGF-GFP, while moving inwardly towards the center of the cell. Once a fibrillar adhesion was stabilized VEGF-GFP showed diffuse accumulation alongside β1 integrin (Fig. 4B, white arrows; Movie 2). VEGF remained associated with stretched fibrillar adhesions and moved passively with them. However, VEGF was rapidly released from integrin + fibers when they collapsed upon mechanical separation from the substrate (Fig. 4C, Movie 2, yellow arrows). These observations are consistent with the hypothesis that astrocytes actively create VEGF-GFP hot spots in their surroundings by actively incorporating VEGF into the assembling fibronectin-containing ECM fibrils. Moreover, the consecutive appearance of integrins and VEGF, and the rapid loss of integrin-VEGF contact upon loss of tension suggests that FN stretching by the integrin/actomyosin system might enhance VEGF/ECM coupling.

To follow the fate of such VEGF-loaded ECM-integrin complexes, we focused on the attaching surface (i.e., attaching to the coverslip) of astrocytes that coexpressed VEGF-GFP and mCherry or β1-SNAP (1.75–7 min/frame), and collected light from a ~2 μm submembraneous band region by pinhole closure. VEGF particles were brighter close to the surface than inside the cell (i.e., below the focus plane), as demonstrated by the weak fluorescence intensity of the Golgi region. Originating at the cell periphery, a retrograde flow of VEGF-GFP was observed, composed of both (1) small, rapidly moving, medium intensity dots (i.e., intracellular vesicles, see Movie 3), and (2) large and bright VEGF-GFP-ECM-β1-SNAP complexes slowly (mean v: 6.89 ± 2.2, max v: 19.95 ± 6.89; μm/h 6 SD) drifting on the surface (Movie 3 and 5, arrows). This later motion was reminiscent of the movement of fibrillar adhesions (Pankov et al., 2000), suggesting the integrin-dependent translocation of VEGF on the surface. Interestingly, the bright, drifting complexes gradually shrank and shifted out of focus (i.e., towards the intracellular space; Fig. 4D, arrowhead in inserts; Movie 3 and 5, arrows), likely indicating endocytic events. Seeking further support for this idea, we analyzed the effect of the dynamin-blocker Dynasore (80 μM) during time-lapse recordings. Despite the absence of retrograde vesicles and VEGF internalizations, Dynasore seemed to stabilize ec. VEGF levels, while after washout of the inhibitor, VEGF-GFP-ECM assembly at adhesions was reinitiated (Movie 4, arrow). Measurements of adhesional GFP intensities confirmed the observed stabilization of VEGF accumulations when comparing Dynasore and control (DMSO) treatments (Supp. Info. Fig. 2). However, stable post-Dynasore GFP intensities may also have reflected the role of dynamin in the trans-Golgi network exit of VEGF-GFP (Jones et al., 1998; McNiven et al., 2000). To separate VEGF secretion from endocytosis a different approach to the question was applied, namely the use of a reversible blockade of protein synthesis with puromycin (10 μg/ml). Time-lapse videos with corresponding whole cell GFP intensities demonstrated a rapid decline in VEGF signal after treatment, and a large steady increase after washout of puromycin (Fig. 4E, Movie 5). This not only shows dependence of VEGF accumulations on continuous delivery but also points to the rapidity of VEGF turnover. Since β1 integrin was SNAP-labeled and hence its signal was not regenerated by de-novo synthesis, the relatively stable SNAP signal was consistent with the efficient recycling of β1 integrin (Fig. 4E; Bretscher, 1989,1992). Therefore, differences observed between the signal of b1-SNAP and VEGF-GFP were indirect signs of both efficient endocytosis and relatively poor recycling of VEGF.

VEGFR2 and NP-1, but Not NP-2 Shows Clustering and Colocalization with VEGF at Cell-Matrix Adhesions

To explore the question whether local VEGF secretion at astrocytic adhesion sites could also be foci of autocrine signaling, we first performed immunofluorescent labeling for VEGFR2, FN, and GFP on astrocytes expressing VEGF-GFP (Fig. 5A). Most VEGFR2+ dots were diffusely scattered in cells, without signs of accumulation or extensive colocalization with VEGF-GFP at the leading edge. However, we also found small clusters of VEGFR2 at FN fibrils (Fig. 5A insert, arrowheads), which frequently colocalized with VEGF-GFP (Fig. 5A, insert, arrowheads). Since VEGFR2 undergoes constant internalization and recycling during signaling (Jopling et al., 2011), this observation was compatible with the idea that VEGF and its receptor are found at these sites with a potential for localized signaling.

NP-1 and 2 have been described as co-receptors that modulate VEGFR2 signaling (Olsson et al., 2006) and enhance VEGF-VEGFR2 binding and VEGF-165 mediated chemotaxis (Soker et al., 1998). Therefore, we next immuno-stained NP-1 and NP-2, and found a dispersed punctate staining much alike to VEGFR2 with both antibodies, which were generally not co-localizing with VEGF-GFP. However, a fraction of NP-1, but not NP-2, also showed considerable clustering and colocalization with VEGF-GFP at FN fibrils (Fig. 5B, arrowheads), while NP-2 distribution was less organized and coincided with VEGF dots only at vesicle-like structures (Fig. 5C, single and double arrowheads, respectively). Although the colocalization between VEGFR2 or NP-1 and VEGF was only partial at FN+ sites, these images raise the possibility that secreted, VEGF recruits and activates VEGFR2/NP-1 complexes at adhesion sites, initiating localized signaling cell-matrix adhesions located at the leading edge of polarized astrocytes.

Knowing that VEGF increases the proliferation of astrocytes (Schmid-Brunclik et al., 2008), and that the mitogenic function of VEGF also requires VEGFR2 activation (Hashimoto et al., 2006; Jin et al., 2002; Keyt et al., 1996; Schanzer et al., 2004), following mitogenic activity could be used to test for the presence of VEGF-GFP/VEGFR2/NP-1 mediated signaling. Therefore, we performed pulse labeling with BrdU in replated VEGF-GFP or GFP transduced cultures. Given that replating increases the proportion of astrocytes in cultures, we have found that BrdU staining was associated almost always with GFAP positivity (Supp. Info. Fig. 3, arrowheads). BrdU+ cell counts among VEGF-GFP+ cells showed that VEGF-GFP nearly doubled the percentage of dividing cells (Fig. 5D, % BrdU in GFP), while the proliferative cellular fraction (Ki67+) remained unchanged (Fig. 5D, % Ki67 in GFP). These data demonstrated that VEGF-GFP was able to accelerate cell cycle in astrocytes (Fig. 5D, % BrdU in Ki67). Taken together the results strongly supported the notion that ECM-bound VEGF signaling acts cell-autonomously on VEGF secreting astrocytes.

Surface-Bound VEGF Decreases β 1 Integrin Turnover at Cell-Matrix Adhesions

To further explore the functional impact of ECM-bound VEGF at cell-matrix adhesions, we aimed to find an alternative read-out that could reflect a local effect of VEGFR2 activation. Previous studies showed that ECM bound VEGF can activate β1 integrins in endothelial cells (Byzova et al., 2000; Chen et al., 2010), breast tumor cells (Goel et al., 2012) and cortical astrocytes also express β1 integrins *in vivo* (Baeten and Akassoglou, 2011; Robel et al., 2009). We hypothesized that the focalized deposition of VEGF could influence the dynamics of astrocytic cell-matrix adhesions. To analyze dynamic properties of adhesions, we cotransduced astrocytes with β 1-SNAP and VEGF-GFP or GFP and compared the mobility of adhesional β1 integrins with FRAP experiments (Fig. 6A; Wehrle-Haller, 2007). We observed that bleaching VEGF loaded adhesions resulted in slower fluorescence recov ery than those of the adhesions of control astrocytes (Fig. 6B, Movie 6, arrows). To quantify integrin turnover, we plotted adhesion-fluorescence in time, and via curve fitting we determined the MF of integrins at each measured adhesion. Averaging data from all reliably fitted adhesions, we found a significantly lower average MF in VEGF-GFP associated junctions (Fig. 6C “ALL”), although, the inclusion of the complete spectrum of ECM adhesions produced considerable variance of recoveries (Wehrle-Haller, 2012). Our efforts

to define more homogenous groups by selecting adhesions based on morphological and dynamic criteria (see Fig. 6 legends) resulted in a decrease of SDs of data points and larger and more significant differences between average MFs when, and even more when adhesions (Fig. 6C). Thus, the expression of VEGF-GFP appears to decrease integrin turnover specifically in mature (“MIDDLE”) or maturing (“SLIDING”) fibrillar adhesions.

To further test whether the effects of VEGF on adhesions is cell-autonomous, we repeated experiments on astrocytes expressing only β1-SNAP, and compared MFs obtained in the same cultures before and after the addition of 200 ng/ ml human recombinant VEGF-165 to the medium. Consistent with a cell-autonomous function of immobilized VEGF, we found that high concentrations of the same VEGF-165 isoform as in VEGF-GFP did not change β1 integrin turnover (Fig. 6D). Thus, the specific deposition of VEGF in the ECM by secreting astrocytes appears to be required for VEGF-mediated stabilization of β1 integrin in cell-matrix adhesions (Fig. 6B), thereby promoting VEGF-b1 integrin crosstalk.

Discussion

In this study, we used a GFP-tagged protein to investigate VEGF trafficking in primary astrocytes. Our results reveal a polarization of VEGF to integrin-mediated cell-matrix adhesion sites. We provide evidence that astrocytes actively integrate VEGF into the ECM on the cell surface where VEGF is colocalized with FN, VEGFR2 as well as NP1 in fibrillar adhesions. Astrocytes appear to distribute VEGF to the environment on the surface of shed membrane protrusions and degrade ECM-bound VEGF via endocytosis. Finally, we show that cell surface-bound, but not soluble VEGF decreases β1 integrin turnover in fibrillar adhesions and propose that VEGF signaling may increase the stability of maturing fibrillar adhesions in a cell autonomous manner. Based on previous and our data, we propose a model of VEGF secretion and active incorporation into the ECM by astrocytes (Fig. 7).

Previous studies indicated that VEGF and its receptors may display a polarized distribution in a variety of cell types including Drosophila wing disc epithelial cells (Rosin et al., 2004), retinal pigment epithelium (Blaauwgeers et al., 1999), astrocytes (Saito et al., 2011), and human endometrial epithelial cells (Hornung et al., 1998). The cellular basis underlying the polarized distribution of VEGF has not been explored previously. To address this issue, we used a lentiviral vector-based approach to introduce the VEGF-GFP fusion protein into polarized astrocytes in primary mixed cultures of neuronal and glial cells. Although lentiviral vectors may infect different cell types in these preparations, the morphological characteristics enabled a clear identification of astroglia. Our video time-lapse as well as *post hoc* analyses revealed for the first time a targeted transport of VEGF towards the leading edge of VEGF-source cells, and demonstrated that VEGF is retained at the cell surface where it is colocalized with FN fibrils at fibrillar adhesions. Earlier studies, demonstrated that VEGF could bind specifically to FN but not to vitronectin or collagen on the surface of endothelial cells (Martino et al., 2011; Wijelath et al., 2006). Moreover, other studies showed that endothelial cells facilitate the immobilization of exogenous VEGF in their surroundings (Köhn-Luque et al., 2013). We extend these observations by directly showing that VEGF progressively accumulates specifically in preformed fibrillar adhesions (Fig. 4B, Movie 2, white arrow) and it is rapidly released from ECM fibrils upon loss of

tension (Fig. 4C, Movie 2, yellow arrows), indicating that active matrix remodeling by astroytes facilitates VEGF immobilization. This latter observation is consistent with the notion that VEGF may bind to the heparin-II domain of FN, which also plays a role in the stabilization of the compact FN conformation (Johnson et al., 1999). It is, therefore, tempting to speculate that the heparin-II domain might be more accessible for VEGF binding in the stretched conformation of FN, leading to an enhanced VEGF/ECM binding upon FN fibrillogenesis. Notion could significantly contribute to the proangiogenic effect of stiff matrices recently observed in breast cancer (Wang et al., 2015). However, the physical link of VEGF/FN complex to cells through integrins was required to promote VEGF-induced endothelial cell proliferation and migration (Wijelath et al., 2006). Moreover, the assembly of the VEGF/ FN complexes is important to direct endothelial tip cell migration in the developing retina (Stenzel et al., 2011), or to enhance wound healing in diabetic conditions (Martino et al., 2011). Thus, the present report along with earlier works strongly supports the idea that FN is a key ECM partner of VEGF in enhancing cellular responses to the growth factor, and VEGF source cells, such as astrocytes have an active role in establishing the connections between matrix molecules and growth factors. In addition, our finding, that only secreted, cell-surface assembled VEGF/FN complexes have affected integrin turnover (Fig. 6C vs. D), also underlines the role of astrocytes in the formation of local VEGF/ FN complexes, that creates synergies with integrin-mediated adhesion and signaling to further enhance the autocrine response to VEGF in astrocytes.

It is also of interest that primary astrocytes, just as COS7 cells (Guzman-Hernandez et al., 2014) were shedding VEGF-covered vesicles (Fig. 3D) from the surface. Our electron microscopic data corroborate and extend, therefore, the observations of Proia et al., who proposed that primary astrocytes shed VEGF containing vesicles, without specifying whether VEGF was inside or on the surface of these structures (Proia et al., 2008). Vesicular shedding could, therefore, represent a specific way to distribute VEGF in a matrix-bound state.

We observed that once associated with FN fibrils on the surface, the VEGF retrograde flow closely matched the speed of myosin-mediated retrograde flow of fibrillar adhesions (Pankov et al., 2000; Zamir et al., 2000), suggesting that VEGF-containing ECM is continuously remodeled by astrocytes. This remodeling also involves efficient internalization and degradation of surface-bound VEGF. Decreased GFP intensity after puromycin (Fig. 4E, Movie 5) indirectly proved the existence and importance of endocytosis and degradation of VEGF in astrocytes. Furthermore, electron microscopic (Fig. 3D) and time-lapse (Fig. 4D, Movie 3) studies point to two separate ways of internalization: peripheral, diffuse endocytosis and peri-centriolar, organized mass-endocytic events. Peripheral VEGF endocytosis might be in part associated to VEGF-VEGFR2 signaling, as the essential role of endocytosis in VEGF signal transduction has been described both regarding caveolae (Liao et al., 2009; Tahir et al., 2009) and clathrin-coated vesicles (Gourlaouen et al., 2013; Lampugnani et al., 2006; Nakayama et al., 2013), while the observed mass internalization/ degradation of ECM-bound VEGF could serve to actively eliminate excess VEGF from the environment. Indeed, during time-lapse experiments we often observed that astrocytes actively collected and removed VEGF-GFP attached to the petri dish (examples in the beginning of Movie 1). Therefore, the combination of targeted secretion and effective

elimination confers a tight bidirectional control over environmental VEGF levels in astrocytes. In consequence, more than being merely a source of VEGF in the brain, astrocytes actively participate in the dynamic reorganization of the ECM and its growth factor composition.

An important aspect of our findings is that targeted VEGF secretion may have a local, autocrine function on VEGF secreting glial cells. The global influence of VEGF on astrocytes has been described in a recent publication showing increased proliferation and process movement after external VEGF-165 treatment (Wuestefeld et al., 2012). Besides showing similarly global consequences of VEGF exposure such as acceleration of the cell cycle (Fig. 5d), the stabilization of β1 integrin in maturing cell-matrix adhesions described by our FRAP studies represents a spatially restricted outcome of targeted VEGF secretion and immobilization (Fig. 6B,C, Movie 6). VEGF co-localization with clusters of VEGFR2/ NP-1 at fibrillar adhesions (Fig. 5A,B) and the increased proliferation after VEGF over-expression (Fig. 5D) suggest local VEGFR2/ NP1 signaling at adhesions. When considering whether a similar signaling could precede also the stabilization of β1 integrins, it is of interest to note that in breast cancer cells it is rather NP-2 that may contribute to integrin activation (Goel et al., 2012). Nevertheless, the proposed mechanism of adhesion stabilization via targeted secretion and immobilization of VEGF could allow to change glial and endothelial functions in specific and spatially restricted manner *in vivo.* Furthermore, integrin-mediated VEGF immobilization and VEGF-mediated integrin stabilization could represent locally restricted, reciprocal interactions leading to VEGF/ECM synergistic signaling to enhance regeneration at sites of injury.

A major unanswered question for future investigation is how the stabilization of integrins might happen? Analysis with γ3-integrins has shown that Rac1 activity slows integrin turnover in cell-matrix attachments sites (Ballestrem et al., 2001). Evidence exists also for reciprocal interactions between VEGFR2 - αvβ3 (Borges et al., 2000; Mahabeleshwar et al., 2007; Papo et al., 2011; Soldi et al., 1999; Traub et al., 2013; West et al., 2012), or VEGFR2 - α5β1 integrins during migration (Wijelath et al., 2002, 2006). The mechanism underlying the replacement of “free” integrins with “built-in” integrins within fibrillar adhesions, however, is unclear. Theoretically, “free” integrins might arrive from an intracellular pool via recycling (Eva et al., 2010, 2012; Powelka et al., 2004), but also from the plasma membrane by diffusion (Rossier et al., 2012). Regulation could be triggered either by VEGFR2 signaling via the promotion of integrin activation (Byzova et al., 2000), which could extend the time course of tripartite interactions (FN/integrin/cytoskeletal adaptors) leading to decreased integrin mobility within the adhesions (Rossier et al., 2012). Nevertheless, mechanisms independent from VEGFR2 signaling may also be present. For instance, NP-1 was shown to interact with β1 integrin (Fukasawa et al., 2007), moreover, it promotes mobilization of integrins from adhesions (Valdembri et al., 2009), therefore an eventual modification of NP-1 functions by interaction with VEGF/ECM complexes could be a mechanism to temper β1 integrin internalization at fibrillar adhesions. Moreover, VEGF can directly bind β1 integrin (Hutchings et al., 2003; Oommen et al., 2011; Vlahakis et al., 2007) and therefore possibly modulate its mobility through molecular interactions.

Regardless of the exact mechanism, our findings uncover a novel, cell-autonomous function of VEGF in secreting astrocytes, and outline a regulatory mechanism of astrocyte polarization and movement. In the brain, this could be particularly important at β1 integrin mediated adhesions that connect astrocytic vascular end feet to perivascular basal membranes (Robel et al., 2009), which in turn would allow local remodeling of the glio-vascular interactions in a spatially restricted manner. Furthermore, injury mediated changes in vascular permeability may provide a local source of plasma FN that could rapidly be used by astrocytes to create a β1-integrin-mediated scaffold for embedding locally produced VEGF, thereby enhancing regeneration and tissue repair (Sakai et al., 2001).

Supplementary Material

Refer to Web version on PubMed Central for supplementary material.

Acknowledgment

Grant sponsor: Swiss National Foundation; Grant number: 31003A_140940/1

The authors wish to thank E. Husi and C. Saadi for histotechnical assistance, the Bioimaging Core Facility team (F. Prodon, O. Brun, and S. Startchik) for their expertise in confocal imaging and computerized image analysis, and M.A. Rapsomaniki and Z. Lygerou for kindly sharing the easy-FRAP software.

References

Argaw AT, Asp L, Zhang J, Navrazhina K, Pham T, Mariani JN, Mahase S, Dutta DJ, Seto J, Kramer EG, Ferrara N, Sofroniew MV, John GR. 2012 Astrocyte-derived VEGF-A drives blood-brain barrier disruption in CNS inflammatory disease. J Clin Invest 122:2454–2468. [PubMed: 22653056]

Ashikari-Hada S, Habuchi H, Kariya Y, Kimata K. 2005 Heparin regulates vascular endothelial growth factor165-dependent mitogenic activity, tube formation, and its receptor phosphorylation of human endothelial cells. Comparison of the effects of heparin and modified heparins. J Biol Chem 280:31508–31515. [PubMed: 16027124]

Baeten KM, Akassoglou K. 2011 Extracellular matrix and matrix receptors in blood-brain barrier formation and stroke. Dev Neurobiol 71:1018–1039. [PubMed: 21780303]

Ballestrem C, Hinz B, Imhof BA, Wehrle-Haller B. 2001 Marching at the front and dragging behind: differential alphaVbeta3-integrin turnover regulates focal adhesion behavior. J Cell Biol 155:1319–1332. [PubMed: 11756480]

Blaauwgeers HG, Holtkamp GM, Rutten H, Witmer AN, Koolwijk P, Partanen TA, Alitalo K, Kroon ME, Kijlstra A, van Hinsbergh VW, Schlingemann RO. 1999 Polarized vascular endothelial growth factor secretion by human retinal pigment epithelium and localization of vascular endothelial growth factor receptors on the inner choriocapillaris. Evidence for a trophic paracrine relation. Am J Pathol 155:421–428. [PubMed: 10433935]

Borges E, Jan Y, Ruoslahti E. 2000 Platelet-derived growth factor receptor beta and vascular endothelial growth factor receptor 2 bind to the beta 3 integrin through its extracellular domain. J Biol Chem 275:39867–39873. [PubMed: 10964931]

Bretscher MS. 1989 Endocytosis and recycling of the fibronectin receptor in CHO cells. Embo J 8:1341–1348. [PubMed: 2527741]

Bretscher MS. 1992 Circulating integrins: alpha 5 beta 1, alpha 6 beta 4 and Mac-1, but not alpha 3 beta 1, alpha 4 beta 1 or LFA-1. Embo J 11:405–410. [PubMed: 1531629]

Byzova TV, Goldman CK, Pampori N, Thomas KA, Bett A, Shattil SJ, Plow EF. 2000 A mechanism for modulation of cellular responses to VEGF: Activation of the integrins. Mol Cell 6:851–860. [PubMed: 11090623]

Carmeliet P, Ruiz de Almodovar C. 2013 VEGF ligands and receptors: Implications in neurodevelopment and neurodegeneration. Cell Mol Life Sci 70: 1763–1778. [PubMed: 23475071]

Chen TT, Luque A, Lee S, Anderson SM, Segura T, Iruela-Arispe ML. 2010 Anchorage of VEGF to the extracellular matrix conveys differential signaling responses to endothelial cells. J Cell Biol 188:595–609. [PubMed: 20176926]

Etienne-Manneville S, Hall A. 2001 Integrin-mediated activation of Cdc42 controls cell polarity in migrating astrocytes through PKCzeta. Cell 106:489–498. [PubMed: 11525734]

Eva R, Crisp S, Marland JR, Norman JC, Kanamarlapudi V, Ffrench-Constant C, Fawcett JW. 2012 ARF6 directs axon transport and traffic of integrins and regulates axon growth in adult DRG neurons. J Neurosci 32:10352–10364. [PubMed: 22836268]

Eva R, Dassie E, Caswell PT, Dick G, ffrench-Constant C, Norman JC, Fawcett JW. 2010 Rab11 and its effector Rab coupling protein contribute to the trafficking of beta 1 integrins during axon growth in adult dorsal root ganglion neurons and PC12 cells. J Neurosci 30:11654–11669. [PubMed: 20810886]

Ferrara N 2002a Role of vascular endothelial growth factor in physiologic and pathologic angiogenesis: Therapeutic implications. Semin Oncol 29:10–14.

Ferrara N 2002b VEGF and the quest for tumour angiogenesis factors. Nat Rev Cancer 2:795–803. [PubMed: 12360282]

Ferrara N 2010 Binding to the extracellular matrix and proteolytic processing: two key mechanisms regulating vascular endothelial growth factor action. Mol Biol Cell 21:687–690. [PubMed: 20185770]

Fukasawa M, Matsushita A, Korc M. 2007 Neuropilin-1 interacts with integrin beta1 and modulates pancreatic cancer cell growth, survival and invasion. Cancer Biol Ther 6:1173–1180. [PubMed: 17726369]

Goel HL, Pursell B, Standley C, Fogarty K, Mercurio AM. 2012 Neuropilin-2 regulates alpha6beta1 integrin in the formation of focal adhesions and signaling. J Cell Sci 125:497–506. [PubMed: 22302985]

Gourlaouen M, Welti JC, Vasudev NS, Reynolds AR. 2013 Essential role for endocytosis in the growth factor-stimulated activation of ERK1/2 endothelial cells. J Biol Chem 288:7467–7480. [PubMed: 23341459]

Guzman-Hernandez ML, Potter G, Egervari K, Kiss JZ, Balla T. 2014 Secretion of VEGF-165 has unique characteristics, including shedding from the plasma membrane. Mol Biol Cell 25:1061–1072. [PubMed: 24501421]

Hashimoto T, Zhang XM, Chen BY, Yang XJ. 2006 VEGF activates divergent intracellular signaling components to regulate retinal progenitor cell proliferation and neuronal differentiation. Development 133:2201–2210. [PubMed: 16672338]

Hayakawa K, Pham LD, Som AT, Lee BJ, Guo S, Lo EH, Arai K. 2011 Vascular endothelial growth factor regulates the migration of oligodendrocyte precursor cells. J Neurosci 31:10666–10670. [PubMed: 21775609]

Hornung D, Lebovic DI, Shifren JL, Vigne JL, Taylor RN. 1998 Vectorial secretion of vascular endothelial growth factor by polarized human endometrial epithelial cells. Fertil Steril 69:909–915. [PubMed: 9591502]

Houck KA, Ferrara N, Winer J, Cachianes G, Li B, Leung DW. 1991 The vascular endothelial growth factor family: Identification of a fourth molecular species and characterization of alternative splicing of RNA. Mol Endocrinol 5: 1806–1814. [PubMed: 1791831]

Huang YF, Yang CH, Huang CC, Hsu KS. 2012 Vascular endothelial growth factor-dependent spinogenesis underlies antidepressant-like effects of enriched environment. J Biol Chem 287:40938–40955. [PubMed: 23074224]

Hutchings H, Ortega N, Plouet J. 2003 Extracellular matrix-bound vascular endothelial growth factor promotes endothelial cell adhesion, migration, and survival through integrin ligation. Faseb J 17:1520–1522. [PubMed: 12709411]

Ijichi A, Sakuma S, Tofilon PJ. 1995 Hypoxia-induced vascular endothelial growth factor expression in normal rat astrocyte cultures. Glia 14:87–93. [PubMed: 7558244]

Jakobsson L, Kreuger J, Holmborn K, Lundin L, Eriksson I, Kjellen L, Claesson-Welsh L. 2006 Heparan sulfate in trans potentiates VEGFR-mediated angiogenesis. Dev Cell 10:625–634. [PubMed: 16678777]

Jin K, Zhu Y, Sun Y, Mao XO, Xie L, Greenberg DA. 2002 Vascular endothelial growth factor (VEGF) stimulates neurogenesis in vitro and in vivo. Proc Natl Acad Sci USA 99:11946–11950. [PubMed: 12181492]

Johnson KJ, Sage H, Briscoe G, Erickson HP. 1999 The compact conformation of fibronectin is determined by intramolecular ionic interactions. J Biol Chem 274:15473–15479. [PubMed: 10336438]

Jones SM, Howell KE, Henley JR, Cao H, McNiven MA. 1998 Role of dynamin in the formation of transport vesicles from the trans-Golgi network. Science 279:573–577. [PubMed: 9438853]

Jopling HM, Howell GJ, Gamper N, Ponnambalam S. 2011 The VEGFR2 receptor tyrosine kinase undergoes constitutive endosome-to-plasma membrane recycling. Biochem Biophys Res Commun 410:170–176. [PubMed: 21539813]

Keyt BA, Berleau LT, Nguyen HV, Chen H, Heinsohn H, Vandlen R, Ferrara N. 1996 The carboxyl-terminal domain (111–165) of vascular endothelial growth factor is critical for its mitogenic potency. J Biol Chem 271:7788–7795. [PubMed: 8631822]

Köhn-Luque A, de Back W, Yamaguchi Y, Yoshimura K, Herrero MA, Miura T. 2013 Dynamics of VEGF matrix-retention in vascular network patterning. Phys Biol 10:066007. [PubMed: 24305433]

Lampugnani MG, Orsenigo F, Gagliani MC, Tacchetti C, Dejana E. 2006 Vascular endothelial cadherin controls VEGFR-2 internalization and signaling from intracellular compartments. J Cell Biol 174:593–604. [PubMed: 16893970]

Learte AR, Forero MG, Hidalgo A. 2008 Gliatrophic and gliatropic roles of PVF/PVR signaling during axon guidance. Glia 56:164–176. [PubMed: 18000865]

Li YN, Pan R, Qin XJ, Yang WL, Qi Z, Liu W, Liu KJ. 2014 Ischemic neurons activate astrocytes to disrupt endothelial barrier via increasing VEGF expression. J Neurochem 129:120–129. [PubMed: 24251624]

Liao WX, Feng L, Zhang H, Zheng J, Moore TR, Chen DB. 2009 Compartmentalizing VEGF-induced ERK2/1 signaling in placental artery endothelial cell caveolae: A paradoxical role of caveolin-1 in placental angiogenesis in vitro. Mol Endocrinol 23:1428–1444. [PubMed: 19477952]

Licht T, Eavri R, Goshen I, Shlomai Y, Mizrahi A, Keshet E. 2010 VEGF is required for dendritogenesis of newly born olfactory bulb interneurons. Development 137:261–271. [PubMed: 20040492]

Licht T, Goshen I, Avital A, Kreisel T, Zubedat S, Eavri R, Segal M, Yirmiya R, Keshet E. 2011 Reversible modulations of neuronal plasticity by VEGF. Proc Natl Acad Sci USA 108:5081–5086. [PubMed: 21385942]

Mahabeleshwar GH, Feng W, Reddy K, Plow EF, Byzova TV. 2007 Mechanisms of integrin-vascular endothelial growth factor receptor cross-activation in angiogenesis. Circ Res 101:570–580. [PubMed: 17641225]

Manoonkitiwongsa PS, Schultz RL, Whitter EF, Lyden PD. 2006 Contraindications of VEGF-based therapeutic angiogenesis: Effects on macrophage density and histology of normal and ischemic brains. Vascul Pharmacol 44:316–325. [PubMed: 16530019]

Margaritescu O, Pirici D, Margaritescu C. 2011 VEGF expression in human brain tissue after acute ischemic stroke. Rom J Morphol Embryol 52:1283–1292. [PubMed: 22203935]

Martino MM, Tortelli F, Mochizuki M, Traub S, Ben-David D, Kuhn GA, Muller R, Livne E, Eming SA, Hubbell JA. 2011 Engineering the growth factor microenvironment with fibronectin domains to promote wound and bone tissue healing. Sci Transl Med 3:100ra89-

McNiven MA, Cao H, Pitts KR, Yoon Y. 2000 The dynamin family of mechanoenzymes: Pinching in new places. Trends Biochem Sci 25:115–120. [PubMed: 10694881]

Nakayama M, Nakayama A, van Lessen M, Yamamoto H, Hoffmann S, Drexler HC, Itoh N, Hirose T, Breier G, Vestweber D, Cooper JA, Ohno S, Kaibuchi K, Adams RH. 2013 Spatial regulation of VEGF receptor endocytosis in angiogenesis. Nat Cell Biol 15:249–260. [PubMed: 23354168]

Nowak DG, Woolard J, Amin EM, Konopatskaya O, Saleem MA, Churchill AJ, Ladomery MR, Harper SJ, Bates DO. 2008 Expression of pro- and anti-angiogenic isoforms of VEGF is differentially regulated by splicing and growth factors. J Cell Sci 121:3487–3495. [PubMed: 18843117]

Olsson AK, Dimberg A, Kreuger J, Claesson-Welsh L. 2006 VEGF receptor signalling - in control of vascular function. Nat Rev Mol Cell Biol 7: 359–371. [PubMed: 16633338]

Oommen S, Gupta SK, Vlahakis NE. 2011 Vascular endothelial growth factor A (VEGF-A) induces endothelial and cancer cell migration through direct binding to integrin {alpha}9{beta}1: identification of a specific {alpha}9{beta}1 binding site. J Biol Chem 286:1083–1092. [PubMed: 21071450]

Pankov R, Cukierman E, Katz BZ, Matsumoto K, Lin DC, Lin S, Hahn C, Yamada KM. 2000 Integrin dynamics and matrix assembly: tensin-dependent translocation of alpha(5)beta(1) integrins promotes early fibronectin fibrillogenesis. J Cell Biol 148:1075–1090. [PubMed: 10704455]

Papo N, Silverman AP, Lahti JL, Cochran JR. 2011 Antagonistic VEGF variants engineered to simultaneously bind to and inhibit VEGFR2 and alphavbeta3 integrin. Proc Natl Acad Sci USA 108:14067–14072. [PubMed: 21825147]

Pichiule P, Chavez JC, Xu K, LaManna JC. 1999 Vascular endothelial growth factor upregulation in transient global ischemia induced by cardiac arrest and resuscitation in rat brain. Brain Res Mol Brain Res 74:83–90. [PubMed: 10640678]

Powelka AM, Sun J, Li J, Gao M, Shaw LM, Sonnenberg A, Hsu VW. 2004 Stimulation-dependent recycling of integrin beta1 regulated by ARF6 and Rab11. Traffic 5:20–36. [PubMed: 14675422]

Proia P, Schiera G, Mineo M, Ingrassia AM, Santoro G, Savettieri G, Di Liegro I. 2008 Astrocytes shed extracellular vesicles that contain fibroblast growth factor-2 and vascular endothelial growth factor. Int J Mol Med 21:63–67. [PubMed: 18097617]

Rapsomaniki MA, Kotsantis P, Symeonidou IE, Giakoumakis NN, Taraviras S, Lygerou Z. 2012 easyFRAP: an interactive, easy-to-use tool for qualitative and quantitative analysis of FRAP data. Bioinformatics 28:1800–1801. [PubMed: 22543368]

Robel S, Mori T, Zoubaa S, Schlegel J, Sirko S, Faissner A, Goebbels S, Dimou L, Gotz M. 2009 Conditional deletion of beta1-integrin in astroglia causes partial reactive gliosis. Glia 57:1630–1647. [PubMed: 19373938]

Rosin D, Schejter E, Volk T, Shilo BZ. 2004 Apical accumulation of the Drosophila PDGF/VEGF receptor ligands provides a mechanism for triggering localized actin polymerization. Development 131:1939–1948. [PubMed: 15056618]

Rossier O, Octeau V, Sibarita JB, Leduc C, Tessier B, Nair D, Gatterdam V, Destaing O, Albiges-Rizo C, Tampe R, Cognet L, Choquet D, Lounis B, Giannone G. 2012 Integrins beta(1) and beta(3) exhibit distinct dynamic nanoscale organizations inside focal adhesions. Nat Cell Biol 14: 1057–1067. [PubMed: 23023225]

Ruhrberg C, Gerhardt H, Golding M, Watson R, Ioannidou S, Fujisawa H, Betsholtz C, Shima DT. 2002 Spatially restricted patterning cues provided by heparin-binding VEGF-A control blood vessel branching morphogenesis. Genes Dev 16:2684–2698. [PubMed: 12381667]

Ruiz de Almodovar C, Coulon C, Salin PA, Knevels E, Chounlamountri N, Poesen K, Hermans K, Lambrechts D, Van Geyte K, Dhondt J, Dresselaers T, Renaud J, Aragones J, Zacchigna S, Geudens I, Gall D, Stroobants S, Mutin M, Dassonville K, Storkebaum E, Jordan BF, Eriksson U, Moons L, D'Hooge R, Haigh JJ, Belin MF, Schiffmann S, Van Hecke P, Gallez B, Vinckier S, Chedotal A, Honnorat J, Thomasset N, Carmeliet P, Meissirel C. 2010 Matrix-binding vascular endothelial growth factor (VEGF) isoforms guide granule cell migration in the cerebellum via VEGF receptor Flk1. J Neurosci 30:15052–15066. [PubMed: 21068311]

Ruiz de Almodovar C, Lambrechts D, Mazzone M, Carmeliet P. 2009 Role and therapeutic potential of VEGF in the nervous system. Physiol Rev 89: 607–648. [PubMed: 19342615]

Ryu JK, Cho T, Choi HB, Wang YT, McLarnon JG. 2009 Microglial VEGF receptor response is an integral chemotactic component in Alzheimer's disease pathology. J Neurosci 29:3–13. [PubMed: 19129379]

Saito T, Shibasaki K, Kurachi M, Puentes S, Mikuni M, Ishizaki Y. 2011 Cerebral capillary endothelial cells are covered by the VEGF-expressing foot processes of astrocytes. Neurosci Lett 497:116–121. [PubMed: 21536099]

Sakai T, Johnson KJ, Murozono M, Sakai K, Magnuson MA, Wieloch T, Cronberg T, Isshiki A, Erickson HP, Fässler R. 2001 Plasma fibronectin supports neuronal survival and reduces brain

injury following transient focal cerebral ischemia but is not essential for skin-wound healing and hemostasis. Nat Med 7:324–330. [PubMed: 11231631]

Salmon P 2013 Generation of human cell lines using lentiviral-mediated genetic engineering. Methods Mol Biol 945:417–448. [PubMed: 23097121]

Schanzer A, Wachs FP, Wilhelm D, Acker T, Cooper-Kuhn C, Beck H, Winkler J, Aigner L, Plate KH, Kuhn HG. 2004 Direct stimulation of adult neural stem cells in vitro and neurogenesis in vivo by vascular endothelial growth factor. Brain Pathol 14:237–248. [PubMed: 15446578]

Schmid-Brunclik N, Burgi-Taboada C, Antoniou X, Gassmann M, Ogunshola OO. 2008 Astrocyte responses to injury: VEGF simultaneously modulates cell death and proliferation. Am J Physiol Regul Integr Comp Physiol 295:R864–73. [PubMed: 18614764]

Shi F, Sottile J. 2008 Caveolin-1-dependent beta1 integrin endocytosis is a critical regulator of fibronectin turnover. J Cell Sci 121:2360–2371. [PubMed: 18577581]

Soker S, Takashima S, Miao HQ, Neufeld G, Klagsbrun M. 1998 Neuropilin-1 is expressed by endothelial and tumor cells as an isoform-specific receptor for vascular endothelial growth factor. Cell 92:735–745. [PubMed: 9529250]

Soldi R, Mitola S, Strasly M, Defilippi P, Tarone G, Bussolino F. 1999 Role of alphavbeta3 integrin in the activation of vascular endothelial growth factor receptor-2. Embo J 18:882–892. [PubMed: 10022831]

Sondell M, Lundborg G, Kanje M. 1999 Vascular endothelial growth factor has neurotrophic activity and stimulates axonal outgrowth, enhancing cell survival and Schwann cell proliferation in the peripheral nervous system. J Neurosci 19:5731–5740. [PubMed: 10407014]

Stenzel D, Lundkvist A, Sauvaget D, Busse M, Graupera M, van der Flier A, Wijelath ES, Murray J, Sobel M, Costell M, Takahashi S, Fassler R, Yamaguchi Y, Gutmann DH, Hynes RO, Gerhardt H. 2011 Integrin-dependent and -independent functions of astrocytic fibronectin in retinal angiogenesis. Development 138:4451–4463. [PubMed: 21880786]

Sun L, Liang C, Shirazian S, Zhou Y, Miller T, Cui J, Fukuda JY, Chu JY, Nematalla A, Wang X, Chen H, Sistla A, Luu TC, Tang F, Wei J, Tang C. 2003 Discovery of 5-[5-fluoro-2-oxo-1,2-dihydroindol-(3Z)-ylidenemethyl]-2,4- dimethyl-1H-pyrrole-3-carboxylic acid (2-diethylaminoethyl)amide, a novel tyrosine kinase inhibitor targeting vascular endothelial and platelet-derived growth factor receptor tyrosine kinase. J Med Chem 46:1116–1119. [PubMed: 12646019]

Tahir SA, Park S, Thompson TC. 2009 Caveolin-1 regulates VEGF-stimulated angiogenic activities in prostate cancer and endothelial cells. Cancer Biol Ther 8:2286–2296. [PubMed: 19923922]

Tolosa L, Mir M, Asensio VJ, Olmos G, Llado J. 2008 Vascular endothelial growth factor protects spinal cord motoneurons against glutamate-induced excitotoxicity via phosphatidylinositol 3-kinase. J Neurochem 105:1080–1090. [PubMed: 18182045]

Traub S, Morgner J, Martino MM, Honing S, Swartz MA, Wickstrom SA, Hubbell JA, Eming SA. 2013 The promotion of endothelial cell attachment and spreading using FNIII10 fused to VEGF-A165. Biomaterials 34:5958–5968. [PubMed: 23683723]

Valdembri D, Caswell PT, Anderson KI, Schwarz JP, Konig I, Astanina E, Caccavari F, Norman JC, Humphries MJ, Bussolino F, Serini G. 2009 Neuropilin-1/GIPC1 signaling regulates alpha5beta1 integrin traffic and function in endothelial cells. PLoS Biol 7:e25. [PubMed: 19175293]

Van Den Bosch L, Storkebaum E, Vleminckx V, Moons L, Vanopdenbosch L, Scheveneels W, Carmeliet P, Robberecht W. 2004 Effects of vascular endothelial growth factor (VEGF) on motor neuron degeneration. Neurobiol Dis 17:21–28. [PubMed: 15350962]

Vlahakis NE, Young BA, Atakilit A, Hawkridge AE, Issaka RB, Boudreau N, Sheppard D. 2007 Integrin alpha9beta1 directly binds to vascular endothelial growth factor (VEGF)-A and contributes to VEGF-A-induced angiogenesis. J Biol Chem 282:15187–15196. [PubMed: 17363377]

Vutskits L, Djebbara-Hannas Z, Zhang H, Paccaud JP, Durbec P, Rougon G, Muller D, Kiss JZ. 2001 PSA-NCAM modulates BDNF-dependent survival and differentiation of cortical neurons. Eur J Neurosci 13:1391–1402. [PubMed: 11298800]

Wang K, Andresen Eguiluz RC, Wu F, Seo BR, Fischbach C, Gourdon D. 2015 Stiffening and unfolding of early deposited-fibronectin increase proangiogenic factor secretion by breast cancer-associated stromal cells. Biomaterials 54:63–71. [PubMed: 25907040]

Wehrle-Haller B 2007 Analysis of integrin dynamics by fluorescence recovery after photobleaching. Methods Mol Biol 370:173–202. [PubMed: 17416995]

Wehrle-Haller B 2012 Assembly and disassembly of cell matrix adhesions. Curr Opin Cell Biol 24:569–581. [PubMed: 22819514]

West XZ, Meller N, Malinin NL, Deshmukh L, Meller J, Mahabeleshwar GH, Weber ME, Kerr BA, Vinogradova O, Byzova TV. 2012 Integrin beta3 crosstalk with VEGFR accommodating tyrosine phosphorylation as a regulatory switch. PLoS One 7:e31071- [PubMed: 22363548]

Wijelath ES, Murray J, Rahman S, Patel Y, Ishida A, Strand K, Aziz S, Cardona C, Hammond WP, Savidge GF, Rafii S, Sobel M. 2002 Novel vascular endothelial growth factor binding domains of fibronectin enhance vascular endothelial growth factor biological activity. Circ Res 91:25–31. [PubMed: 12114318]

Wijelath ES, Rahman S, Namekata M, Murray J, Nishimura T, Mostafavi-Pour Z, Patel Y, Suda Y, Humphries MJ, Sobel M. 2006 Heparin-II domain of fibronectin is a vascular endothelial growth factor-binding domain: Enhancement of VEGF biological activity by a singular growth factor/matrix protein synergism. Circ Res 99:853–860. [PubMed: 17008606]

Wuestefeld R, Chen J, Meller K, Brand-Saberi B, Theiss C. 2012 Impact of vegf on astrocytes: Analysis of gap junctional intercellular communication, proliferation, and motility. Glia 60:936–947. [PubMed: 22431192]

Zachary I 2005 Neuroprotective role of vascular endothelial growth factor: Signalling mechanisms, biological function, and therapeutic potential. Neurosignals 14:207–221. [PubMed: 16301836]

Zamir E, Geiger B. 2001 Molecular complexity and dynamics of cell-matrix adhesions. J Cell Sci 114:3583–3590. [PubMed: 11707510]

Zamir E, Katz M, Posen Y, Erez N, Yamada KM, Katz BZ, Lin S, Lin DC, Bershadsky A, Kam Z, Geiger B. 2000 Dynamics and segregation of cell-matrix adhesions in cultured fibroblasts. Nat Cell Biol 2:191–196. [PubMed: 10783236]

Zhang H, Vutskits L, Pepper MS, Kiss JZ. 2003 VEGF is a chemoattractant for FGF-2-stimulated neural progenitors. J Cell Biol 163:1375–1384. [PubMed: 14691144]

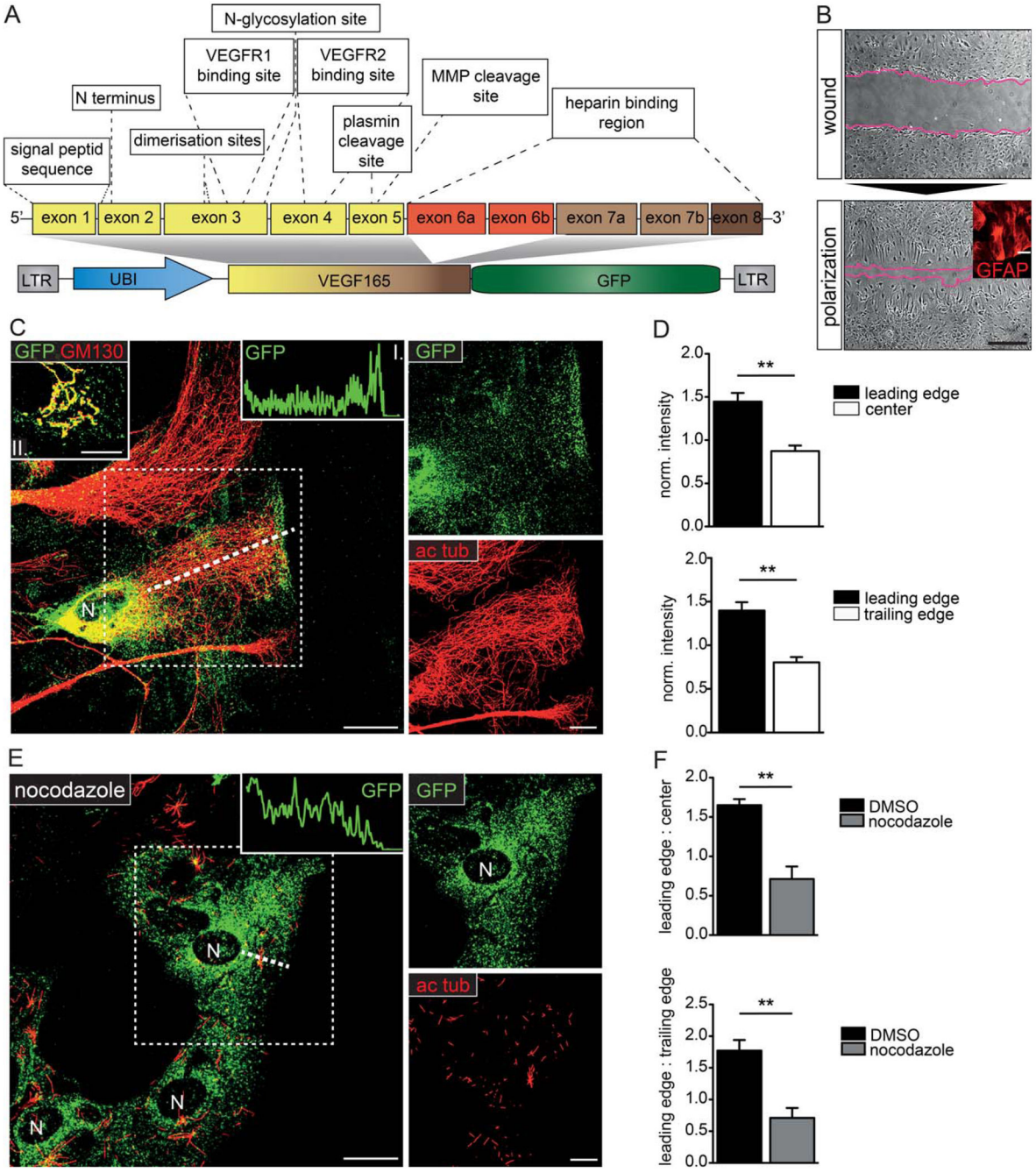

FIGURE 1:

VEGF shows a vectorial distribution in polarized primary astrocytes. **A**: Simplified structure of VEGF-A (based on Nowak et al., 2008), and the VEGF-GFP lentivector (Guzman-Hernandez et al., 2014), which contains the ubiquitin promoter followed by the C-terminal end of (exon 1-7b, except 6a/b) fused to EGFP. LTR, long terminal repeat; VEGFR1 and 2, VEGF receptor 1 and 2. **B**: Phase contrast images of a primary cortical culture, immediately and 24 h after wounding. Astrocytes at the wound edge are polarized and express GFAP (insert). Bars: 100 μm (main image), 50 μm (insert). **C**: Confocal images of VEGF-GFP

transduced, wound-edge astrocytes immunostained for acetylated tubulin (ac tub), and GFP demonstrate that VEGF-GFP accumulates at the Golgi and at the leading edge. Note the intact microtubules. Insert I shows GFP intensity along the dashed line; insert II shows VEGF in the Golgi (GM130). **D**: Statistical comparison of average GFP intensities at leading edge, (non-Golgi) center, and trailing edge regions of random, wound-edge astrocytes prove that polarized VEGF distribution is common among wound-edge cells. mean ± S.E.M., $n = 3$, 81 cells from 3 experiments; unpaired t test ** $P<0.01$. **E**: Confocal images of VEGF-GFP transduced, wound-edge astrocytes stained as in (C) after 1 μg/ml nocodazole. Inhibited microtubule polymerization and cell polarization alters VEGF distribution, which decreases in intensity towards the wound (insert). **F**: Quantification of average normalized regional intensity ratios (leading edge/center and leading edge/trailing edge) between randomly chosen wound-edge cells from control (DMSO) and nocodazole cultures. mean ± S.E.M., control: (D), nocodazole: $n = 3$, 80 cells from 3 experiments; unpaired t test ** $P<0.01$. Bars: 20 μm (main image), 10 μm (close up) (see also Supp. Info. Fig. 1)

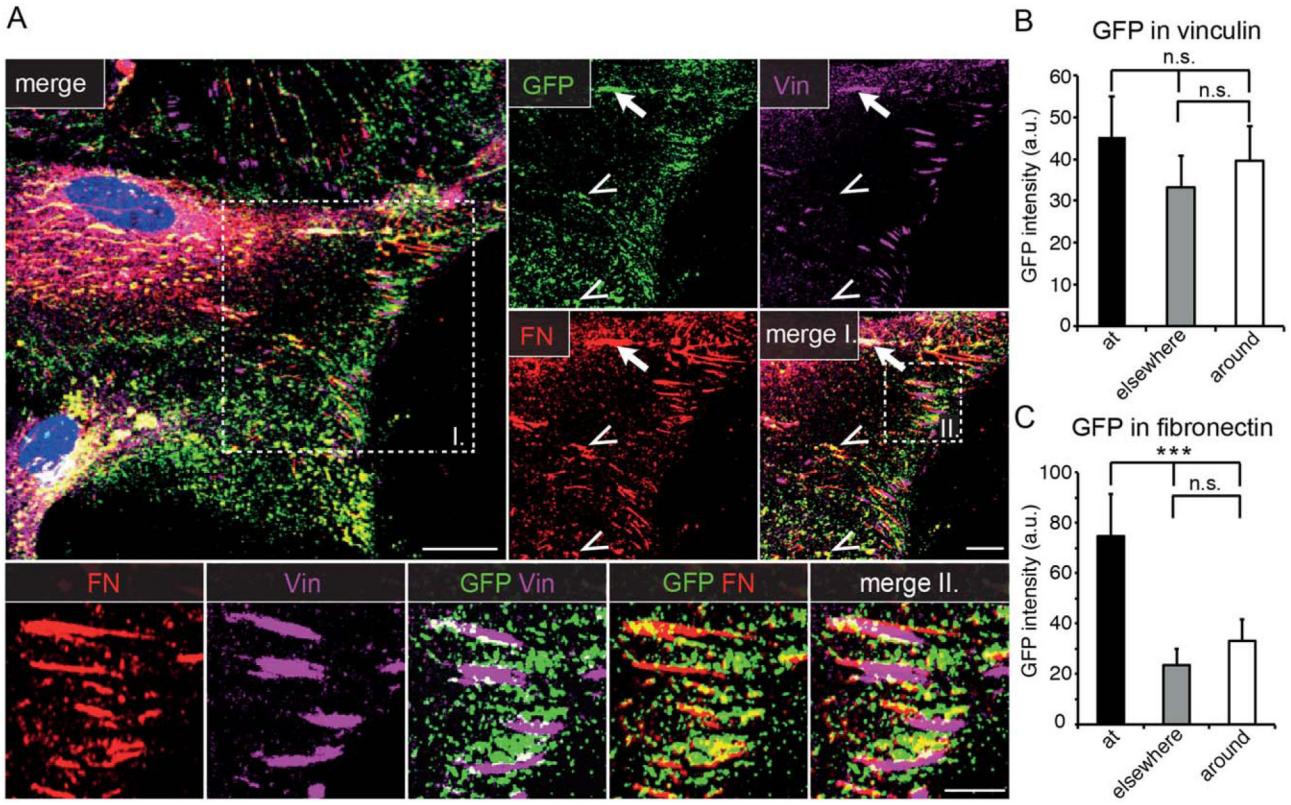

FIGURE 2:

VEGF-GFP is directed to cell-matrix adhesions. **A**: Confocal images of VEGF-GFP transduced, polarized astrocytes stained for markers of focal (vinculin, Vin) and fibrillar adhesions (fibronectin, FN) show that VEGF accumulates mainly in the vicinity of fibrillar adhesions and colocalizes with FN (insert I, arrowheads) or both with FN and Vin (insert I, arrow). Bars: 20 μm (main), 10 μm (insert I), and 5 μm (insert II). **B**: Comparison of average GFP intensity "at" Vin+ regions, 3 μm "around" or "elsewhere" in the cells, suggests a tendency for association to focal adhesions. a.u., arbitrary units, mean ± SEM, 70 cells from 3 experiments, repeated measures ANOVA and Bonferroni post-test, n.s.: nonsignificant difference. **C**: Average GFP intensity is significantly higher "at" FN+ regions than 3 μm "around" or "elsewhere," indicating that VEGF associates preferentially to fibrillar adhesions. Mean ± SEM, 70 cells from 3 experiments, repeated measures ANOVA and Bonferroni post-test *** $P<0.001$; a.u., arbitrary units

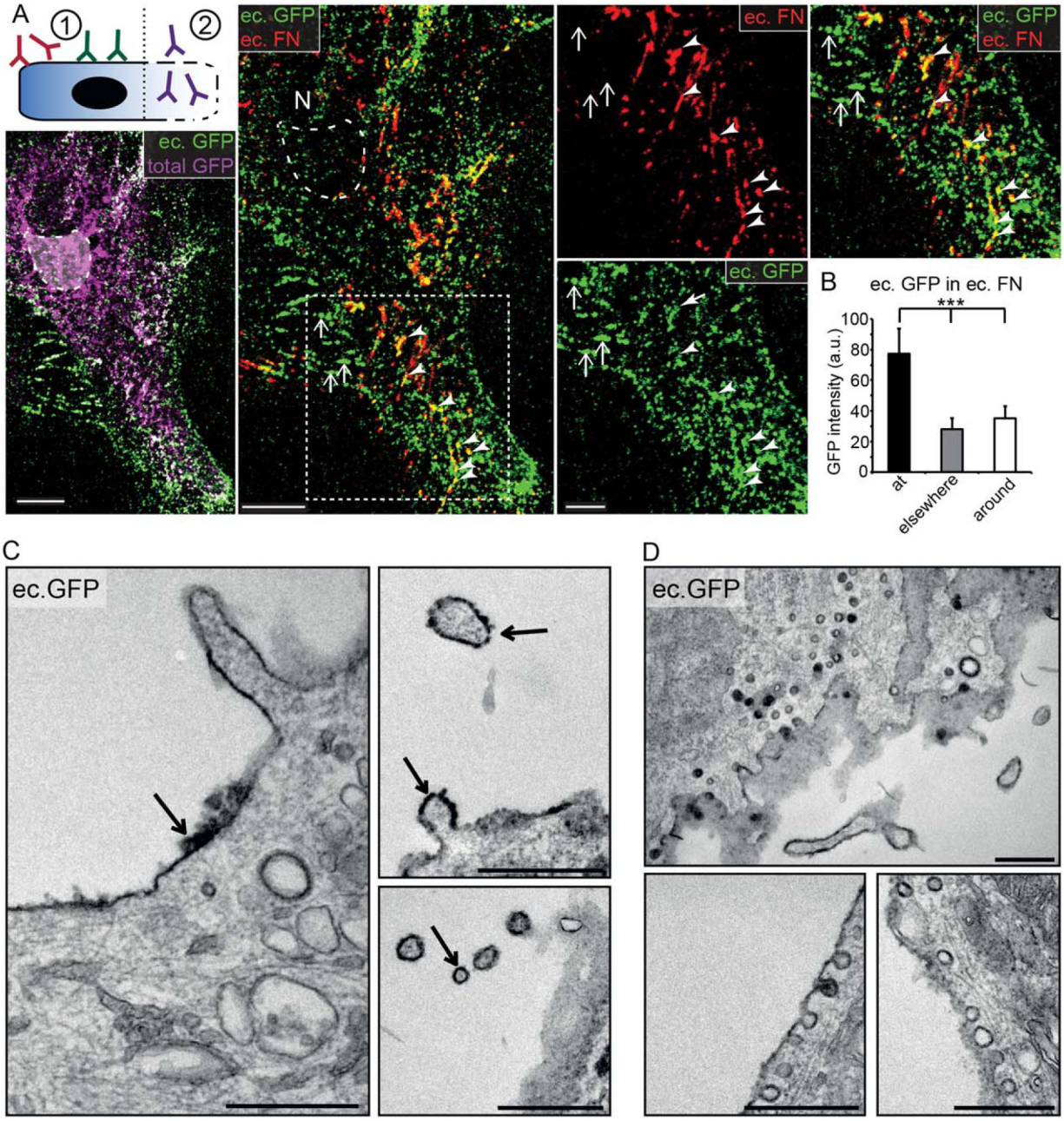

FIGURE 3:

VEGF-GFP accumulates on the cell surface and associates with shedding and endocytic vesicles. **A**: Schematic of intra- and with two-step immunostaining: (1) ec. GFP and FN are labeled with antibodies applied on living cells on ice; (2) following fixation/permeabilization total GFP is labeled with anti-GFP antibodies from a third species. Maximum intensity projected confocal images show that ec. and total GFP widely overlap, while the lack of ec. GFP staining in the Golgi area (dashed line) confirms the specificity of intraextracellular discrimination. VEGF (ec. GFP) accumulates and colocalizes with FN (ec. FN) on the ec. surface (arrow heads). At intercellular junctions (arrows) ec. VEGF-GFP is not accompanied by ec. FN. Bars: 10 μm (main images) and 5 μm (close up). **B**: Quantification of average ec.

GFP intensity showed similar results as in Fig. 2C, suggesting that VEGF and FN associates on the cell surface. Mean ± SEM, 60 cells from 3 experiments, repeated measures ANOVA and Bonferroni post-test *** $P<0.001$; a.u., arbitrary units. **C**: Pre-embedding, DAB immunolabeling of VEGF-GFP transduced astrocytes with externally applied anti-GFP antibodies (as in A). Electron micrographs demonstrate that ec. VEGF accumulates directly on the cell surface (left image, arrow); moreover, it also covers shed vesicles (right images, arrows). Bars: 0.5 μm. **D**: If living cells were washed and placed back to 37°C to allow proper cellular behavior after antibody incubation, endocytosis of surface deposited VEGF was seen. Bars: 0.5 μm.

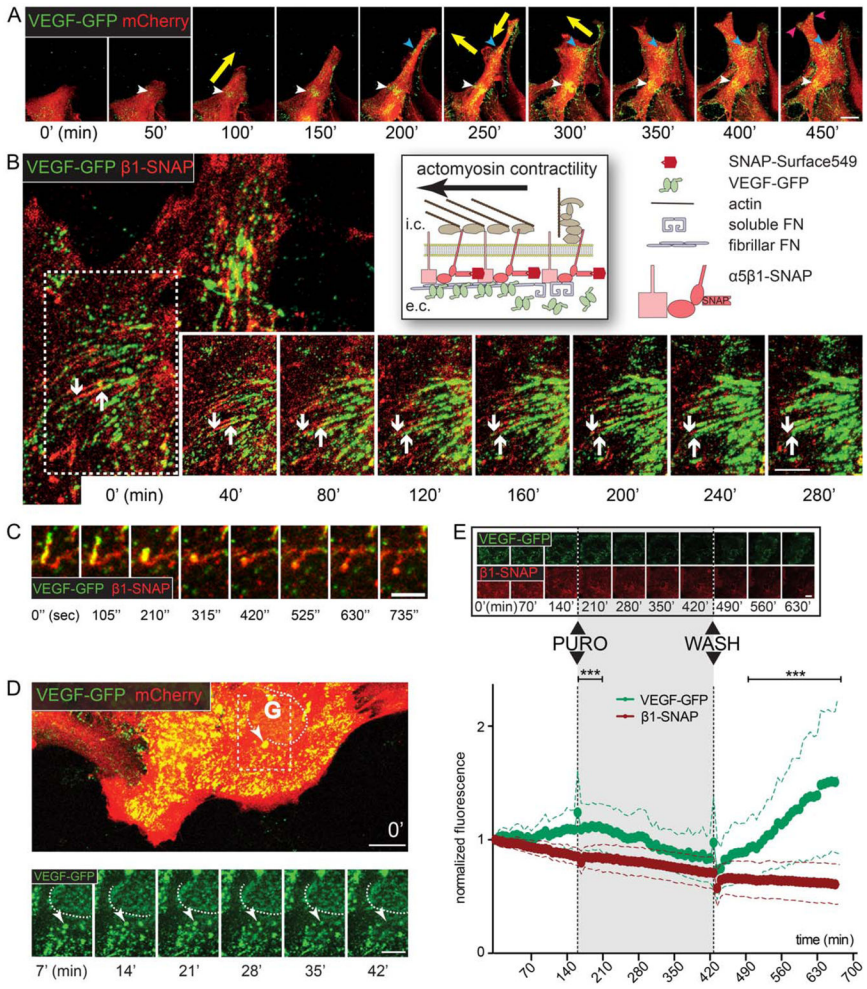

FIGURE 4:

Dynamics of VEGF-GFP in actively assembling ECM. **A**: Sequential confocal time-lapse images (50 min; Movie 1) of an mCherry – VEGF-GFP cotransduced wound-edge astrocyte demonstrate that VEGF accumulates dynamically at cellular attachment points (colored arrowheads). Note the synchronization between the appearance of VEGF and the changing direction of cell movement (yellow arrows). Bar: 20 μm. **B**: Schematic of live-stained β1-SNAP integrins in heterodimers and VEGF-GFP during ECM-remodeling on the right. Sequential confocal time-lapse images (40 min intervals; white arrow in Movie 2) of an attachment point of an astrocyte coexpressing VEGF-GFP and β1-SNAP. Downward arrow points at the central end of an adhesion, upward arrow highlights the limit of propagating VEGF-GFP. VEGF-GFP expands inwards along the growing adhesions, and linear VEGF accumulations are formed, demonstrating that astrocytes actively organize growth factor concentrations in their surroundings by linking VEGF-GFP and the remodeled ECM. Bar: 10 μm. **C**: Cropped image sequence from the same video demonstrates that collapsing adhesions lose their VEGF content (yellow arrows in Movie 2). **D**: Sequential (7 min) confocal time-lapse images (Movie 3) of VEGF-GFP/mCherry cotransduced astrocytes. Near the Golgi (G, dashed line, its weak intensity is due to intracellular localization) a bright and slow (i.e., surface-bound) VEGF-GFP aggregate (arrowhead) gradually shifts out of

focus (i.e., toward intracellular space), depicting the endocytosis of VEGF/ECM complexes. Bars: 20 μm (main) and 10 μm (sequence). **E**: Sequential confocal time-lapse images (70 min, Movie 5) of an astrocyte coexpressing VEGF-GFP/β1-SNAP show the reversible effect of translation blocking with puromycin (PURO, 10 μg/ml). Bar: 20 μm. Measured whole cell average intensities of such experiments are plotted in time, error bars represent SDs (VEGF-GFP is corrected for bleaching). In contrast to GFP, the intensity of β1-SNAP remained fairly stable during the experiments, indicating its efficient recycling and independence from translation. The substantial differences between the two proteins point out that VEGF accumulation is highly dependent on protein synthesis, and that VEGF is degraded after secretion. 52 cells from 3 experiments, two-way ANOVA with Bonferroni post-test *** $P<0.001$ (see also Supp. Info. Fig. 2).

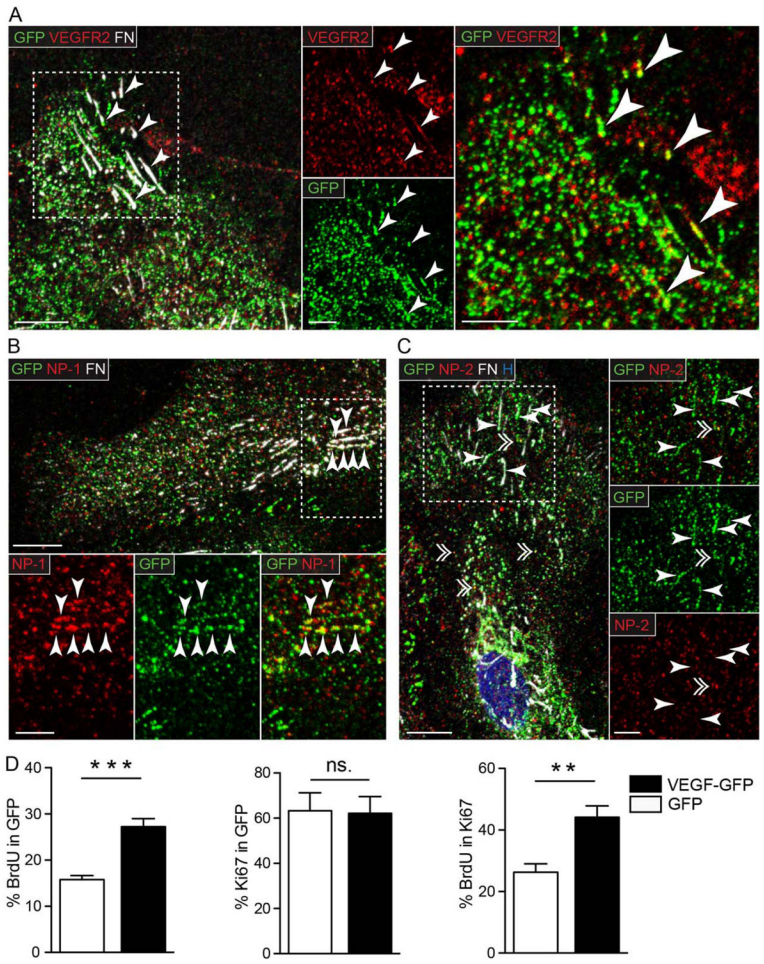

FIGURE 5:

VEGFR2 and NP-1 but not NP-2 shows clustering and colocalization with VEGF-GFP at cell-matrix adhesions. Representative confocal images of astrocytes expressing VEGF-GFP immunostained for GFP, FN and (**A**) VEGF receptor 2 (VEGFR2), or its coreceptors (**B**) neuropilin-1 (NP-1), and (**C**) neuropilin-2 (NP-2). All three proteins had a diffuse, dot-like distribution in the cells, and additionally, VEGFR2 and NP-1 formed linear clusters at FN+ adhesions (arrowheads in A and B), while NP-2 did not (arrowheads in C). Colocalization between VEGF-GFP and VEGFR2 or NP-1 was restricted mainly to linear clusters at cell-matrix adhesions (arrowheads in A and B), while NP-2 occasionally colocalized with VEGF-GFP in vesicle-like structures (double arrowhead in C). H, Hoechst; Bars: 10 μm (main) and 5 μm (close up). **D**: Quantifications following BrdU pulse labeling of subconfluent cultures in serum free medium demonstrated more BrdU+ cells among astrocytes expressing VEGF-GFP than in control GFP cells (% BrdU in GFP). The proliferative fraction (% Ki67 in GFP) was equal at both conditions, meaning that the cell cycle was accelerated by VEGF-GFP (% BrdU in Ki67). This mitogenic effect suggests the presence of VEGFR2 signaling initiated by VEGF-GFP in astrocytes. $n = 6$, unpaired t test, ** $P<0.01$, *** $P<0.001$ (see also Supp. Info. Fig. 3)

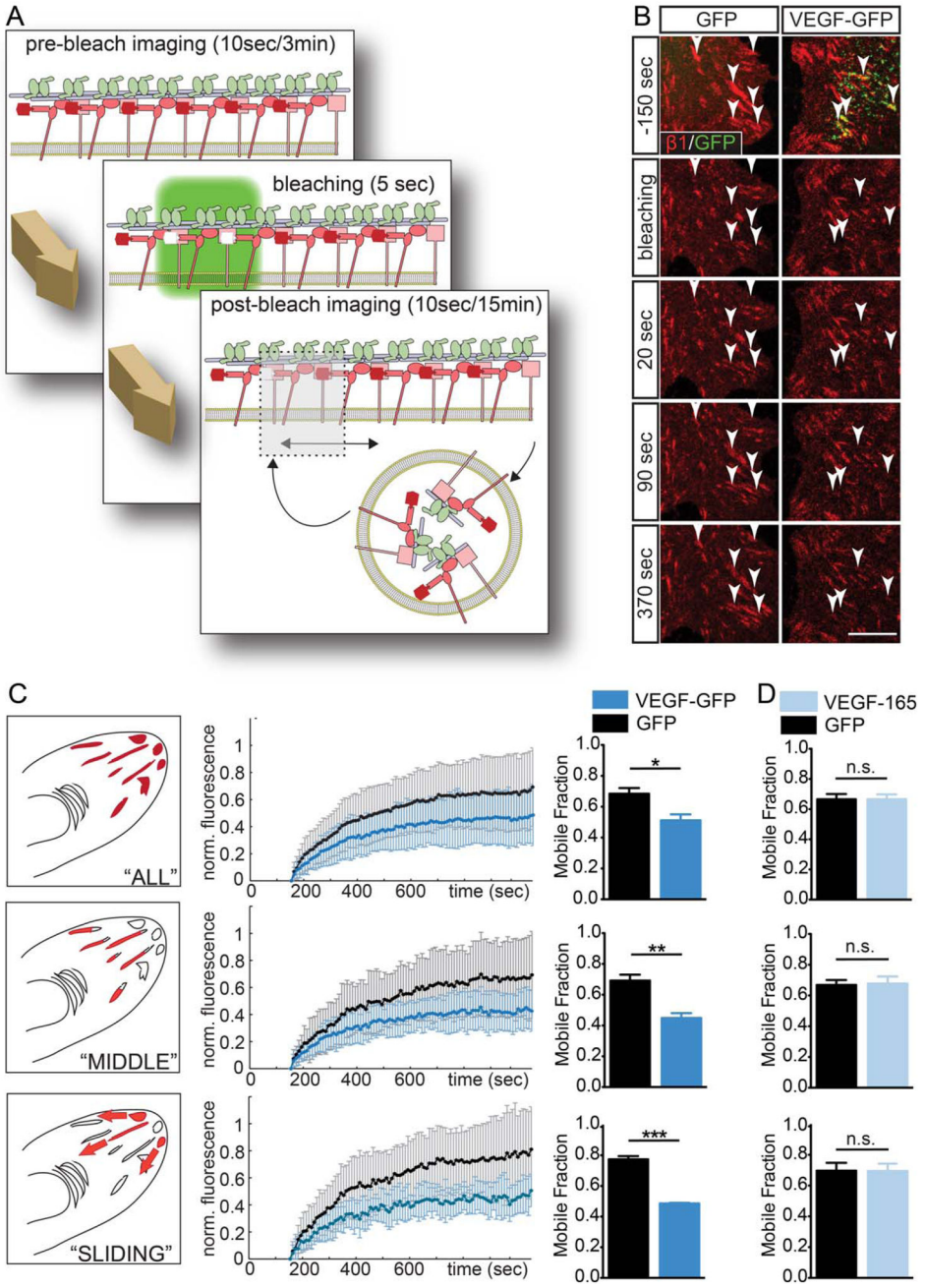

FIGURE 6:

Surface-bound VEGF decreases β1 integrin turnover in an autocrine manner. **A**: Schematic overview of FRAP experiments. **B**: Sequential confocal images from FRAP videos on astrocytes coexpressing β1-SNAP/GFP or VEGF-GFP (Movie 6) demonstrate a weaker integrin recovery in VEGF-loaded adhesions (right column) than in control adhesions (left column). Arrowheads point to bleached areas. Bar: 10 μm. **C**: Average fractional fluorescence recovery curves and corresponding MFs of "ALL" reliably fitted adhesions show that VEGF significantly tempers integrin turnover. Selecting for "MIDDLE" adhesions (axial ratio >5, distance from cell border >3 μm, front part excluded), or "SLIDING"

adhesions (inward extension during experiment) shortened error bars (SD), and differences between MFs became more significant, suggesting that VEGF stabilizes integrins specifically in these mature or maturing cell-matrix adhesions. (n = 4 for “ALL” and “MIDDLE,” 3 for “SLIDING,” control and experimental adhesions: 82, 96; 25, 23; 28, 14; resp.; columns: mean ± SEM; unpaired t test, * P<0.05, ** P<0.01, *** P<0.001). **D**: When FRAP data from control cells before and after addition of VEGF-165 (200 ng/ml) was compared, no difference was observed between mean MFs, suggesting that cellular secretion confers an autocrine effect on adhesions to VEGF. N = 3, control and experimental adhesions: 155, 230; 111, 174; 56, 28; respectively; paired t test; n.s., nonsignificant.

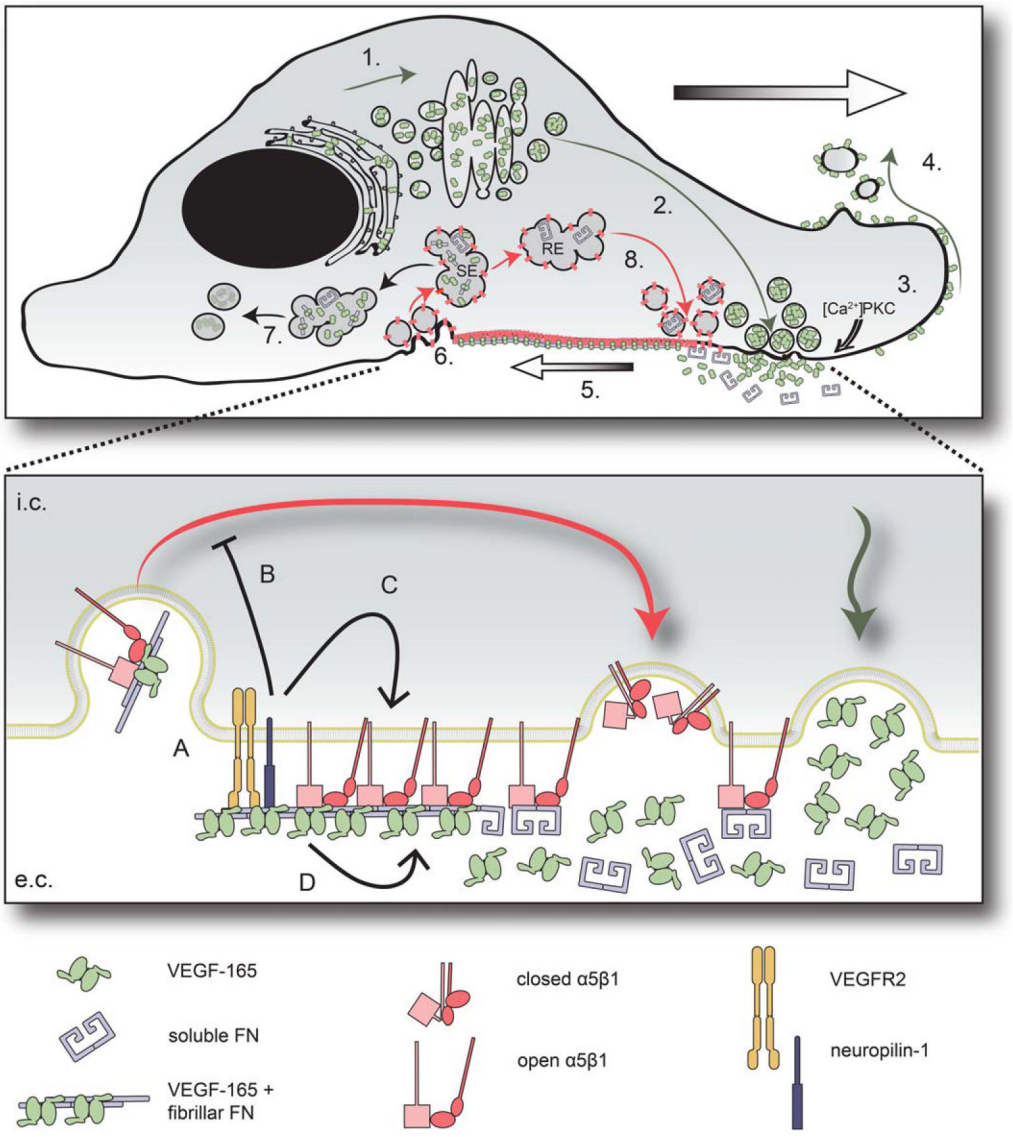

FIGURE 7:

Model of targeted secretion, active matrix deposition of VEGF and its functions in astrocytes. (1) VEGF is translated in the rough endoplasmic reticulum and undergoes post-translational modifications in the Golgi (Guzman-Hernandez et al., 2014). (2) Postgolgi secretory vesicles target apical plasma membrane. (3) VEGF-165 is secreted upon local [Ca2+] increase or protein kinase C (PKC) activation (Guzman-Hernandez et al., 2014), and being sequestered in the ECM, it remains fixed to the membrane. (4) Surface-bound VEGF-165 covers shedding microvesicles. (5) α5β1 integrin heterodimers bind FN and are pulled inward by actomyosin contraction. Cytoskeletal tension transmitted on. FN leads to FN fibrillogenesis, which promotes VEGF-165/FN binding and VEGF-165 incorporation into FN fibrils. (6) VEGF-165/FN complexes and integrin heterodimers are internalized and targeted to a sorting endosomal compartment (SE). (7) VEGF is directed to degradation, while (8) part of FN (Shi and Sottile, 2008) and α5β1 integrins (Bretscher, 1989) are recycled to the surface (red arrows; recycling endosome - RE). The magnification

demonstrates the possible molecular interactions at the level of fibrillar adhesions. **A**: VEGFR2 and neuropilin-1 are clustered to the adhesions and mediate VEGF-165 signal transduction. This signaling leads to decreased β1 integrin turnover in maturing cell-matrix adhesions. The direct mechanism may be (**B**) inhibition of β1 integrin endocytosis/recycling, (**C**) stabilization of β1 integrin in the adhesions by promoting open conformation, or (**D**) direct VEGF-165/integrin interaction leading to integrin stabilization.